Proceedings of the
Annual Stability Conference
Structural Stability Research Council
Louisville, Kentucky, April 13-16, 2021

Local buckling of steel plates supported unilaterally by concrete infill of C-PSW/CF

Joshua R. Harmon[1], Amit H. Varma[2]

Abstract

This paper presents an analytical study on local buckling of steel faceplates in concrete-filled composite plate shear walls (C-PSW/CF). To analyze steel faceplate buckling, concrete infill was considered to be a rigid, tensionless (unilateral) support and shear anchors and tie bars were considered to be point braces. A classical, differential equation, eigenvalue buckling analysis cannot directly solve a buckling problem with a unilateral support. Therefore, an iterative method of solving the unilateral buckling problem with a classical, differential equation, eigenvalue approach was developed and used to study buckling of steel faceplates. The buckling study considered the number of anchor points over the wall height and the unilateral buckling analysis directly incorporated the effects of bracing stiffness. A minimum brace stiffness was found which prevented buckling of the entire faceplate away from the concrete infill; however, a greater brace stiffness was required to develop the faceplate yield strength. Considering an initial out-of-straightness in the steel faceplate, a dual strength and stiffness requirement for tie bars and shear anchors to develop the yield strength of the faceplate in C-PSW/CF was developed. The proposed requirement would accompany the existing design requirements for tie bars and/or shear connectors.

1. Introduction

Concrete-filled composite plate shear walls (C-PSW/CF) are a form of composite construction consisting of steel faceplates connected by steel tie bars and infilled with plain concrete. Shear anchors connect the steel faceplates to the concrete infill. The construction method for C-PSW/CF generally involves shop fabrication of steel modules consisting of the steel faceplates, tie bars, and shear anchors. The steel modules are then transported to the field, erected, and filled with concrete. The shop fabrication of the steel modules and ability of the steel modules to serve as the concrete formwork offer advantages to construction schedule efficiency, can increase construction tolerances of the steel fabrication, and eliminates rebar congestion.

Tie bars provide lateral stability to the empty steel modules prior to concrete casting. Varma et al. (2019) studied the lateral stability of the empty steel modules, creating a design requirement for the tie bar diameter (d_{tie}) and tie bar spacing (S_{tie}). After concrete casting, tie bars and shear anchors

[1] Graduate Research Assistant, Purdue University, <harmon30@purdue.edu>
[2] Karl H. Kettelhut Professor of Civil Engineering, Purdue University, <ahvarma@purdue.edu>

connect the steel faceplates to the concrete infill: (i) creating composite action, and (ii) stabilizing the steel plates against local flexural buckling under compressive stresses. Zhang et al. (2014, 2020) studied local flexural buckling of steel faceplates; creating a maximum tie bar and shear anchor spacing (s) to faceplate thickness (t_p) ratio as a design requirement. Stability bracing design in AISC 2016 is based on a dual brace strength and stiffness requirement, following Winter (1958). The work by Zhang et al. (2014, 2020) did not elaborate on bracing design requirements for shear anchors and tie bars nor establish the governing buckling mode of steel faceplates.

This paper presents a flexural buckling analysis of steel faceplates, identifies the governing buckling mode, and considers the effects of an initial out-of-straightness in the faceplate to create strength and stiffness requirements for tie bars and shear anchors. The strength and stiffness requirements proposed in this paper work in conjunction with the maximum s/t_p ratio created by Zhang et al. (2014, 2020) to allow the steel faceplates to develop the yield stress of the faceplate material.

Throughout this paper, elements which anchor the steel faceplate to the concrete infill and provide interfacial shear transfer between the concrete infill and steel plate are called shear anchors. Headed stud anchors (shear studs) are a commonly used example of a shear anchor. However, other shear anchors may be conceived; thus, the generic term, shear anchor, is used throughout the discussion.

2. Previous Research and Design Requirements

2.1 Shear Buckling of Empty Steel Modules

Before concrete infill has been cast, the steel faceplates are subjected to axial loads from self-weight and construction loads. The empty steel modules are shear flexible and are susceptible to shear buckling under axial loads (Varma et al. 2019). The critical buckling load for a shear flexible structure is equal to the effective shear stiffness of the structure; thus, the buckling load does not depend upon boundary conditions or unbraced length. Varma et al. proposed limiting the buckling load of the empty steel modules to a minimum of 1000psi. With an expression for the effective shear stiffness of the steel modules, the proposed minimum buckling load creates a design requirement for a maximum tie bar spacing to faceplate thickness ratio which depends upon the tie bar diameter, as given in Eq. 1.

$$\frac{S_{tie}}{t_p} \leq 1.0\sqrt{\frac{E}{2\alpha+1}} \tag{1}$$

where, S_{tie} is the tie bar spacing, t_p is the faceplate thickness, E is the modulus of elasticity, and α is the relative flexural stiffness of the tie bar with respect to the steel faceplate, see Eq. 2.

$$\alpha = 1.7\left(\frac{t_p}{d_{tie}}\right)^3\left(\frac{T_{sc}-t_p}{d_{tie}}\right) \tag{2}$$

where, t_p is the faceplate thickness, d_{tie} is the tie bar diameter, and T_{sc} is the thickness of the composite wall.

2.2 Local Buckling of Steel Faceplates

Local buckling of steel faceplates for C-PSW/CF occurs such that the steel faceplate buckles away from the concrete infill under compressive stress. Zhang et al. (2014, 2020) compiled a database of experimental compression tests on C-PSW/CF specimens with shear studs used as the shear anchors. The range of plate slenderness ratio (s/t_p) in the database ranged from 15 to 100 and the normalized plate slenderness ratio$\left(s/t_p \cdot \sqrt{F_y/E}\right)$ ranged from 0.5 to 3.9, where F_y is the yield stress of the faceplate. The test database is represented in Fig.1 as the normalized buckling strain (buckling strain divided by the material yield strain) on the ordinate and the normalized plate slenderness ratio on the abscissa. Zhang et al. (2014) found the data to follow a buckling effective length factor of 0.7 for normalized buckling strain less than 0.6; however, Zhang et al. (2020) confirmed that the mean buckling effective length factor was 0.8.

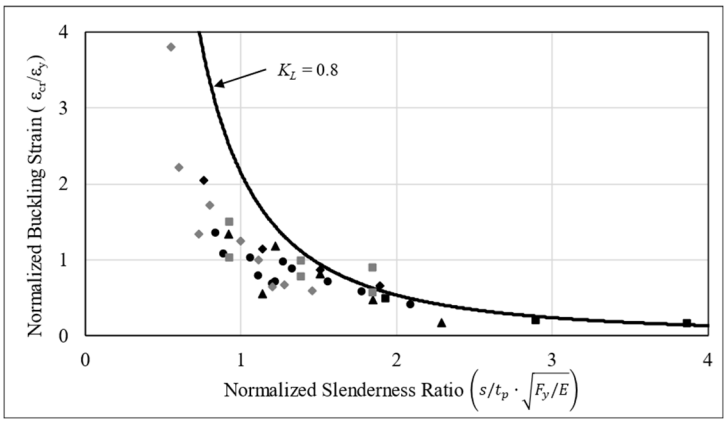

Figure 1: Experimental C-PSW/CF local buckling test database. Adapted from Zhang et al. (2020).

Because there were no test results with normalized buckling strain less than 1.0 for a normalized slenderness ratio less than 1.0, Zhang et al. (2014) interpreted this to mean that yielding in compression occurred before local buckling when the normalized slenderness ratio was less than 1.0. Zhang et al. used this observation to develop the requirement for the faceplates to be non-slender, i.e., undergo compression yielding prior to local buckling. the design requirement states that the normalized slenderness ratio must be less than 1.0, see Eq. 3.

$$\frac{s}{t_p} \leq 1.0\sqrt{\frac{E}{F_y}} \tag{3}$$

where, s is the spacing between shear anchors and tie bars, t_p is the faceplate thickness, E is the modulus of elasticity, and F_y is the faceplate yield stress.

The work by Zhang et al. (2014) or Zhang et al. (2020) does not establish the governing buckling mode of steel faceplates for C-PSW/CF. It does state that buckling occurs between adjacent rows of shear anchors and a photograph of a compressively loaded C-PSW/CF specimen in Zhang et al. (2020) shows local buckling of the faceplate extending over two adjacent rows of shear studs.

2.3 Basis for Bracing Design

Winter (1958) studied column bracing design; creating a dual strength and stiffness requirement for bracing which remains the basis of AISC (2016) brace design requirements. Winter (1958)

studied a column of length $2L$, with "pinned" ends, moment of inertia I, and a brace of stiffness K at midspan, see Fig. 2. The authors of this paper solved for the bifurcation buckling load of this column with a classical, differential equation, eigenvalue method presented by Galambos and Surovek 2008. The solution method is for linear, elastic materials; assumes a constant cross-section with no initial imperfections; and enforces boundary conditions of zero displacement and bending moment at supports, equilibrium of shear at the midspan brace, and continuity of displacement, rotation, and bending moment at the midspan brace. The column buckling modes for $K = 0$ are also shown in Fig. 2. Fig. 3 shows the value of the column buckling load as a function of the brace stiffness for the first and second buckling modes. The column buckling load is normalized by the Euler buckling load for the unbraced length, $P_E = \pi^2 \cdot E \cdot I / L^2$, and the brace stiffness is a normalized value: $K \cdot L^3 / (E \cdot I)$

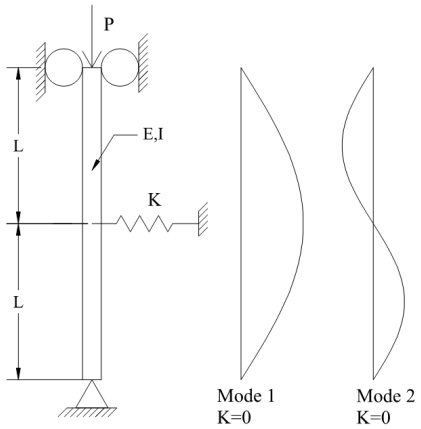

Figure 2: "Pinned" column with midspan brace from Winter 1958.

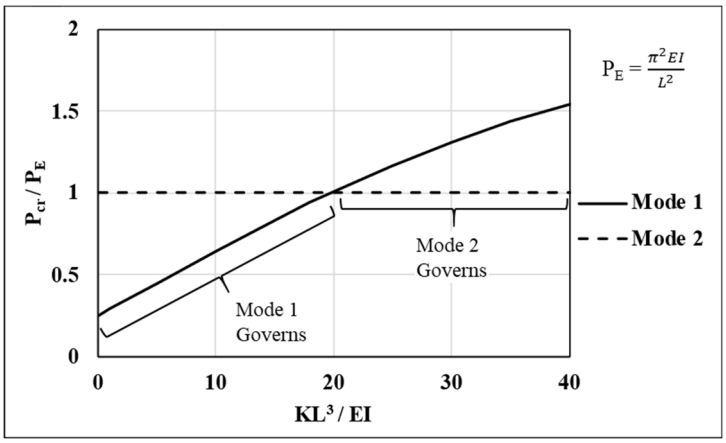

Figure 3: Buckling load versus brace stiffness of Winter 1958 column.

Winter (1958) targeted a column buckling load equal to the Euler buckling load between brace points; thus, the ideal brace stiffness is the brace stiffness where the governing buckling load becomes equal to P_E. Coincidentally, the ideal brace stiffness is also the value of the brace stiffness where the first mode buckling load becomes greater than the second mode buckling load. Hence, the second mode becomes the governing buckling mode for brace stiffness values greater than the ideal brace stiffness, for this column. The ideal brace stiffness for this column is $19.77 \cdot E \cdot I / L^3$, which can also be written as $2 \cdot P_E / L$.

The column studied by Winter (1958) assumes a "perfect" column without initial imperfections. An initial out-of-straightness and other imperfections exist in any real column. To account for imperfections, Winter (1958) modeled an initial out-of-straightness (Δ_0) at mid-span of the column. With the imperfection included in the analysis, the required brace stiffness to reach the Euler buckling load increased as Δ_0 increased and the required brace stiffness decreased as the allowable deflection during loading (Δ) increased. If Δ and Δ_0 were equal, the required brace stiffness was twice the ideal brace stiffness. The required brace strength was the required brace stiffness multiplied by Δ.

The principles of the strength and stiffness requirements for bracing design from Winter (1958) appear in AISC (2016). The targeted buckling load for columns in AISC (2016) is the same as for Winter (1958): the Euler buckling load for the unbraced length. The ideal brace stiffness for a column with multiple equally spaced point braces approaches $4 \cdot P_E / L$. The AISC (2016) stiffness requirement corresponds to twice the ideal brace stiffness. The required brace stiffness in AISC is $8 \cdot P_r / L$, where P_r is the axial load demand of the column. Winter (1958) states $L/500$ can be taken as the allowable column deflection after loading; thus, the required brace strength for the column considered by Winter (1958) is $2 \cdot (2 \cdot P_E / L) \cdot (L / 500) = 0.008 \cdot P_E$. The AISC (2016) required strength is increased from the required strength found by Winter (1958) to account for additional brace forces due to member curvature and member continuity across brace points (AISC 2016). The required column brace strength in AISC (2016) is $0.01 \cdot P_r$.

3. Buckling Analysis of Steel Faceplates

To conduct a buckling analysis of steel faceplates for C-PSW/CF, the faceplates were modeled as an axially loaded column. Restraint to the faceplate at the ends of the C-PSW/CF due to boundary elements was not considered; allowing a tributary width of the faceplate to be considered for the analysis. Restraint to the faceplate due to shear anchors, tie bars, and concrete infill was included in the analysis. Shear anchors and tie bars were considered to be anchors, or point braces, restraining buckling of the faceplate away from the concrete infill. The anchors were modeled as linear, elastic springs with axial stiffness, K, and were evenly spaced along the height of the column. The concrete infill was considered to be rigid, undeformable, in compression, preventing the faceplate from buckling into the concrete infill but providing no restraint against buckling away from the concrete infill. The concrete infill was modeled a rigid, tensionless support: a unilateral restraint. A complementarity eigenvalue method (Sio et al. 2017) could be used to perform a buckling analysis with unilateral restraints; however, an alternative method was used in this study through the evaluation of buckling mode shapes and introduction of additional supports to the column model to represent contact of the faceplate with the concrete infill. The details of this method will be discussed later in the paper.

Three column configurations are discussed in detail to determine the effect of the number of shear anchors over the height of the faceplate. Models FF-1A, FF-2A, and FF-3A model "fixed" ended columns with 1, 2, and 3 intermediate point braces, respectively. "FF" refers to the "fixed" ends of the columns. The results of the buckling analysis are then applied to a column with numerous braces.

3.1 Unilateral Restraint Buckling Analysis Procedure

The buckling analysis of the column models was initially completed by omitting the unilateral restraint of the concrete infill and considering only the restraint due to the point braces. With the buckling mode shape from the initial analysis, additional supports were added to the column model to represent the restraint of the concrete infill.

The column buckling analyses treated the column models as a "perfect", elastic column: linear, elastic material behavior, no initial imperfections, and constant cross-section. An eigenvalue problem was created by applying boundary conditions to equations for the buckled shape of the column, following Galambos and Surovek (2008). The equations for the buckled shape were obtained from Bernoulli-Euler beam theory. The boundary conditions used in the solution were zero displacement and rotation at supports, equilibrium of shear at the intermediate braces, and continuity of displacement, rotation, and moment at the intermediate braces. The eigenvalue problem was solved as a function of the brace stiffness.

For each brace stiffness value of each column buckling mode, the buckled mode shape of the column was evaluated in incorporating the unilateral restraint. If the buckling analysis resulted in the column buckling to only one side of the un-deformed column configuration, the unilateral restraint had been satisfied and no further analysis was required. If the buckled shape of the column was on both sides of the un-deformed column configuration, the unilateral restraint had not been satisfied and further analysis was required.

The unilateral restraint adds constraint to the buckled shape of the column; therefore, considering the unilateral restraint in the buckling analysis cannot reduce the buckling load of the column below the buckling load obtained by omitting the unilateral restraint. The buckling load obtained by omitting the unilateral restraint is thus a lower bound for the column buckling load with the unilateral restraint. The lower bound buckling load for higher order (second order or higher) buckling modes is used in this paper when the lower bound buckling load is greater than the governing buckling load. The governing buckling load is the smallest buckling load from all buckling modes at a given brace stiffness.

The buckled shape for some buckling modes satisfied the unilateral restraint for all brace stiffness values and for some buckling modes the buckled shape violated the unilateral restraint for all brace stiffness values. For other buckling modes, the buckled shape satisfied the unilateral restraint for a brace stiffness of zero and violated the unilateral restraint as the brace stiffness increased. For example, the first buckling mode for FF-2A initially satisfied the unilateral restraint but the mode shape buckled into the concrete infill in two locations as the brace stiffness increased, as shown in Fig. 8. Because the unilateral restraint is rigid in compression and offers no restraint in tension, the unilateral restraint allows the column to either remain straight and un-deformed or to buckle away from the concrete infill above and below the point of contact between the concrete infill and steel faceplate. Regardless of which of these behaviors would occur, this support condition was modeled by adding a "fixed" support, zero displacement and zero rotation, to the column model, which could be moved, or slid, along the length of the column. The sliding "fixed" support divided the column into separate column buckling analysis problems above and below the sliding support, see Fig. 8.

For FF-2A, sliding "fixed" supports were added to the column model for the eigenvalue buckling analysis in both regions where the initial mode shape buckled into the concrete infill. The location of the added supports was determined iteratively. The added supports were moved towards the middle of the column until the buckling mode shape no longer violated the unilateral restraint. As the brace stiffness increased, the additional supports moved towards the braced points of the column. As previously mentioned, the addition of the moving "fixed" supports divided the column into separate buckling analysis problems. Each section of the column, above and below the additional support, must be considered to determine the buckling load of the entire column. For FF-2A, the middle segment of the column always governed the buckling load. However, the middle segment is not guaranteed to govern the buckling load and buckling of each segment must be considered.

The iterative process described above was used to locate the position of the additional "fixed" supports in the model which represent contact between the steel faceplate and the concrete infill. With the additional supports, the eigenvalue buckling analysis could determine the buckling load of the column while incorporating the unilateral restraint. The iterative analysis was used to solve the buckling load for the first buckling mode of FF-2A and FF-3A. The second buckling mode of the column was also solved with the iterative process, when the lower bound buckling load solution for the second buckling mode was less than first mode buckling load solution.

3.2 FF-1A: Column with One Anchor

Fig. 4(a) shows the column model FF-1A, representing a steel faceplate with one intermediate anchor bracing the faceplate against flexural buckling. The column has a rectangular cross-section with depth of the faceplate thickness, t_p, and a tributary width resulting in moment of inertia, I. Three buckling modes from the eigenvalue buckling analysis are shown for zero brace stiffness in Fig. 4. Mode 1 and mode 3 satisfied the unilateral restraint without additional analysis, for zero brace stiffness. The mode shape for mode 3 did not depend upon the brace stiffness and mode 3 satisfied the unilateral restraint for all brace stiffness values. When the brace stiffness increased such that the mode 1 buckling load became greater the mode 3 buckling load, the mode shape for mode 1 no longer satisfied the unilateral restraint. The mode 1 buckling load solution shown in Fig. 6 for buckling loads greater than the mode 3 buckling load are a lower bound solution. This distinction is inconsequential; as will be discussed later, mode 2 was the governing buckling load for this region of brace stiffness values.

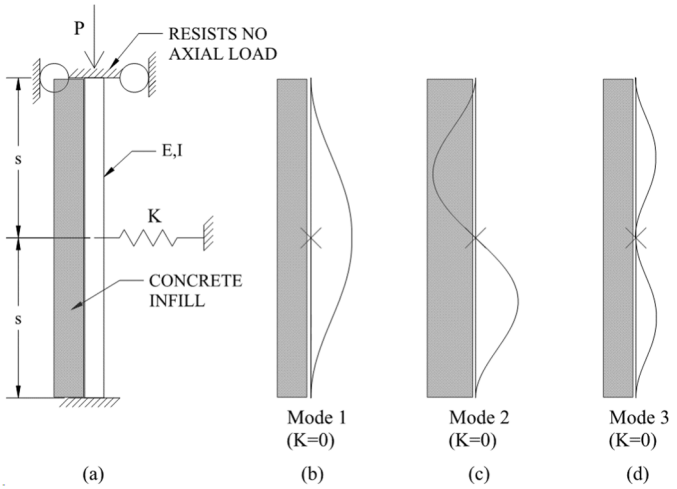

Figure 4: Column model for FF-1A with buckling modes.

Mode 2 did not satisfy the unilateral restraint for any brace stiffness value and additional analysis was required. For brace stiffness K=0, a moving "fixed" support was added to the column model such that the buckling load of the column with the added support and the second mode buckling load of the column without the added support were equal, see Fig. 5(a). As the brace stiffness was increased, the additional support was slid along the length of the column until buckling occurred away from the concrete infill and the unilateral restraint was satisfied, see Fig. 5(b). The iteratively determined mode 2 buckling load was referred to as the mode 2 – iterative solution, which accounts for both restraint due to the shear anchors and restraint due to contact between the steel faceplate and concrete infill.

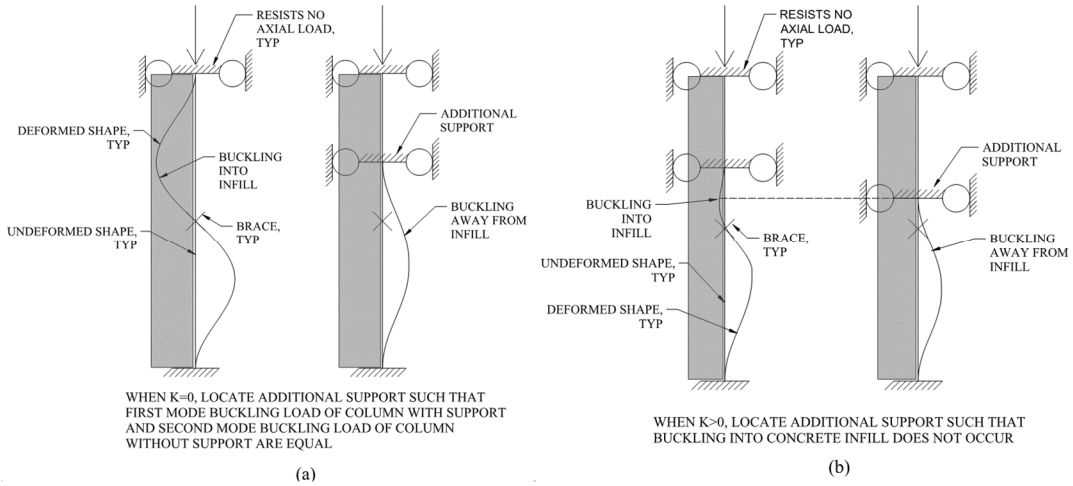

Figure 5: Second mode iterative buckling analysis for FF-1A.

The results of the buckling analysis for FF-1A are summarized in Fig. 6. Fig. 6 shows the normalized critical buckling load: P_{cr} / P_E, where P_E is the Euler buckling load between brace points: $P_E = \pi^2 \cdot E \cdot I / s^2$, on the ordinate and the normalized brace stiffness: $K \cdot s^3 / (E \cdot I)$, on the abscissa. As the brace stiffness increases, the governing buckling load increases, but cannot exceed the mode 3 buckling load. The mode shape for mode 3 is constant as the brace stiffness varies and has a constant buckling load of $4 \cdot P_E$. For mode 2 – iterative, the buckling load is $2 \cdot P_E$ for zero brace stiffness, corresponding to the buckling mode shown in Fig. 4(c) and 5(a), and increases

with increasing brace stiffness, but does not exceed the mode 3 buckling load. Fig. 6 concludes that the governing buckling load for FF-1A is governed by mode 1 for $K < 34 \cdot E \cdot I / s^3$ and is governed by mode 2 – iterative for $K \geq 34 \cdot E \cdot I / s^3$.

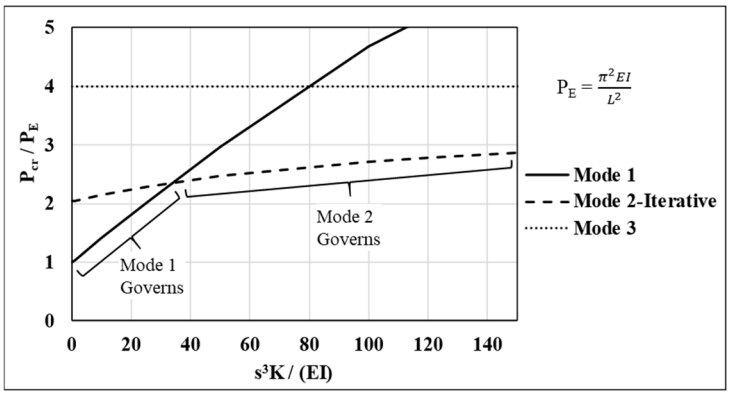

Figure 6: Buckling load versus brace stiffness for FF-1A.

3.3 FF-2A: Column with Two Anchors

Fig. 7(a) shows the column model FF-2A, representing a steel faceplate with two intermediate anchors bracing the faceplate against flexural buckling. The column has a rectangular cross-section with depth of the faceplate thickness, t_p, and a tributary width resulting in moment of inertia, I. Five buckling modes from the eigenvalue buckling analysis are shown for zero brace stiffness in Fig. 7. Mode 3 and mode 5 satisfied the unilateral restraint without additional analysis, for all brace stiffness values analyzed. Mode 2 and mode 4 did not satisfy the unilateral restraint for any brace stiffness; however, as will be shown, the lower bound buckling loads for these two buckling modes were greater than the mode 1 buckling load which satisfied the unilateral restraint. The lower bound solution was used for mode 2 and mode 4, without additional analysis. The buckling solution for mode 2 and mode 4 were termed the mode 2 - lower bound and mode 4 – lower bound solutions, respectively.

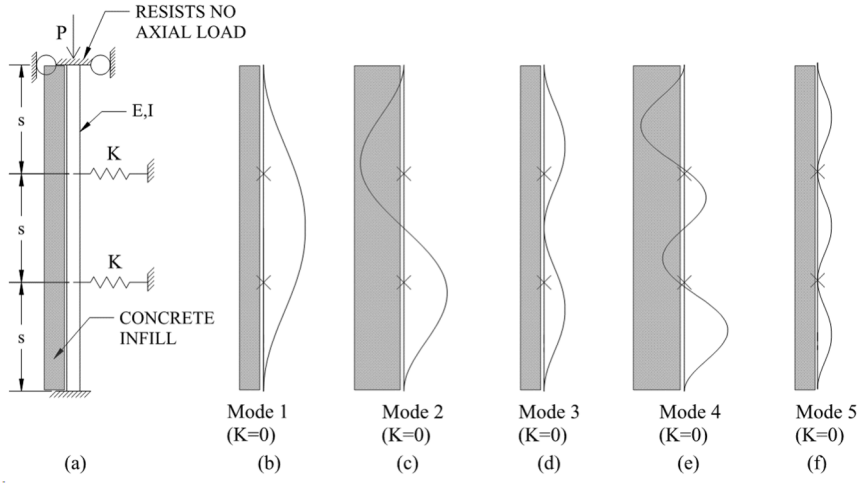

Figure 7: Column model for FF-2A with buckling modes.

For mode 1, with zero brace stiffness, the entire length of the faceplate buckled away from the concrete infill, as shown by the mode shape in Fig. 7(b). As the brace stiffness increased, the

faceplate buckled into the concrete infill in two locations, as shown in Fig. 8, violating the unilateral restraint. Two sliding "fixed" supports were added to the column model to represent contact between the faceplate and the concrete infill. The additional supports were iteratively moved along the length of column until buckling into the concrete infill did not occur. The buckling solution from this analysis is termed the mode 1 - iterative solution.

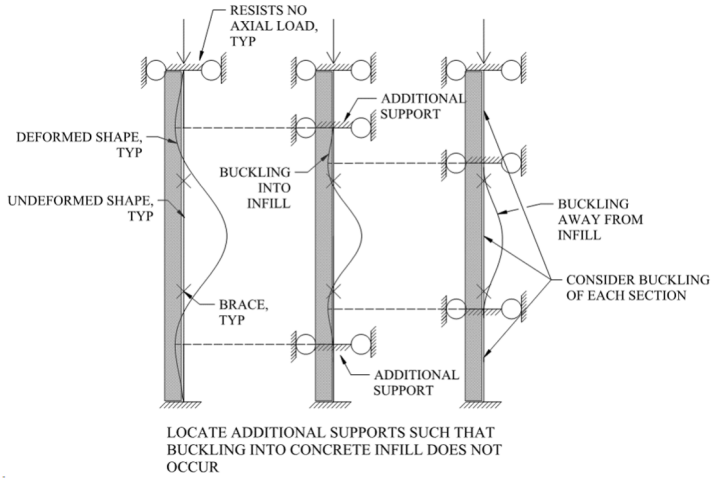

Figure 8: First mode iterative buckling analysis for FF-2A.

The results of the buckling analysis for FF-2A are summarized in Fig. 9. Fig. 9 shows the normalized critical buckling load: P_{cr} / P_E, where P_E is the Euler buckling load between brace points: $P_E = \pi^2 \cdot E \cdot I / s^2$, on the ordinate and the normalized brace stiffness: $K \cdot s^3 / (E \cdot I)$, on the abscissa. The buckling load for mode 4 and mode 5 are approximately constant as the brace stiffness varies. The mode 1 – iterative buckling load solution is the governing buckling load for all brace stiffness values. As the brace stiffness increases, the governing buckling load increases, but does not exceed the mode 2 – lower bound buckling load nor the mode 4 – lower bound buckling load. If the unilateral restraint were enforced for the mode 2 and mode 4 solutions, the mode 2 – lower bound and mode 4 – lower bound solutions would increase, but not affect the governing buckling load. Fig. 9 concludes that the governing buckling load for FF-2A is governed by mode 1 for all brace stiffness, the buckling load exceeds P_E for $K \geq 10 \cdot E \cdot I / s^3$, and exceeds $2 \cdot P_E$ for $K \geq 100 \cdot E \cdot I / s^3$.

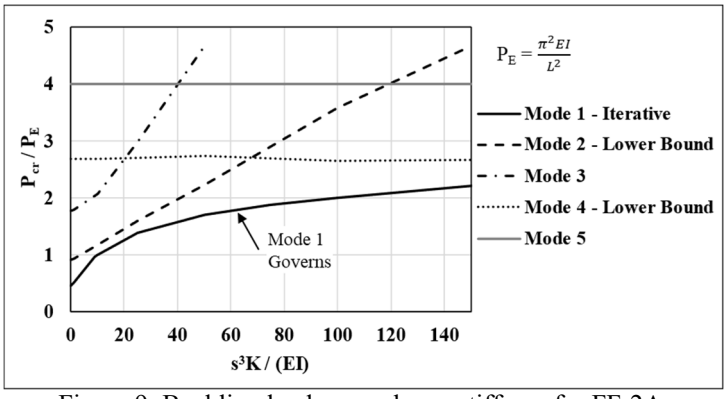

Figure 9: Buckling load versus brace stiffness for FF-2A.

3.4 FF-3A: Column with Three Anchors

Fig. 10(a) shows the column model FF-3A, representing a steel faceplate with three intermediate anchors bracing the faceplate against flexural buckling. The column has a rectangular cross-section with depth of the faceplate thickness, t_p, and a tributary width resulting in moment of inertia, I. Seven buckling modes from the eigenvalue buckling analysis are shown for zero brace stiffness in Fig. 10. Mode 5 and mode 7 satisfied the unilateral restraint without additional analysis, for all brace stiffness values analyzed. Mode 2, mode 4, and mode 6 did not satisfy the unilateral restraint for any brace stiffness. Additional analysis to satisfy the unilateral restraint for mode 2 was completed, as will be discussed later. The lower bound buckling load solution was used for mode 3, mode 4, and mode 6. As shown later, the mode 1 and mode 2 buckling load solutions considering the unilateral restraint govern the buckling load of the column and thus the buckling solution satisfying the unilateral restraint for mode 3, mode 4, and mode 6 would be inconsequential. The buckling solution for mode 3, mode 4, and mode 6 are termed the mode 3 - lower bound, mode 4 – lower bound, and mode 6 – lower bound solutions, respectively. For mode 1 with zero brace stiffness, the entire length of the faceplate buckled away from the concrete infill. As the brace stiffness increased, the faceplate buckled into the concrete infill in two locations, violating the unilateral restraint in a similar way to that seen by mode 1 for FF-2A. Two sliding "fixed" supports were added to the column model to represent contact between the faceplate and the concrete infill. The additional supports were iteratively moved along the length of column until buckling into the concrete infill did not occur. The buckling solution from this analysis is termed the mode 1 - iterative solution.

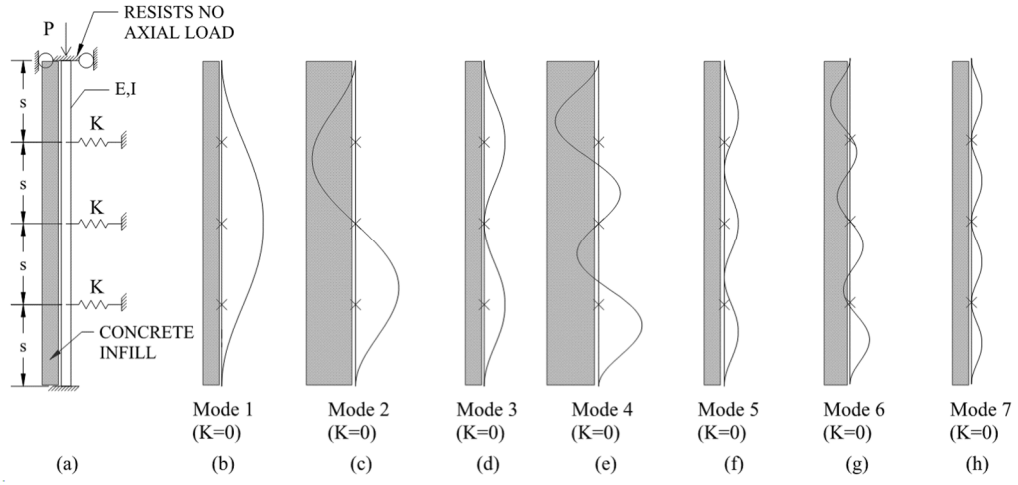

Figure 10: Column model for FF-3A with buckling modes.

Mode 2 did not satisfy the unilateral restraint for any brace stiffness value and additional analysis was required. For brace stiffness K = 0, a moving "fixed" support was added to the column model such that the buckling load of the column with the added support and the second mode buckling load of the column without the added support were equal, see Fig. 11(a). As the brace stiffness was increased, the additional support was slid along the length of the column until buckling occurred away from the concrete infill and the unilateral restraint was satisfied, see Fig. 11(b). As the brace stiffness increased further, buckling into the concrete infill occurred at the opposite end of the column from where the additional support was previously added. Another moving support was added to the model to reflect restraint from the concrete infill at both ends of the column, see

Fig. 11(b). The iteratively determined mode 2 buckling load was referred to as the mode 2 – iterative solution.

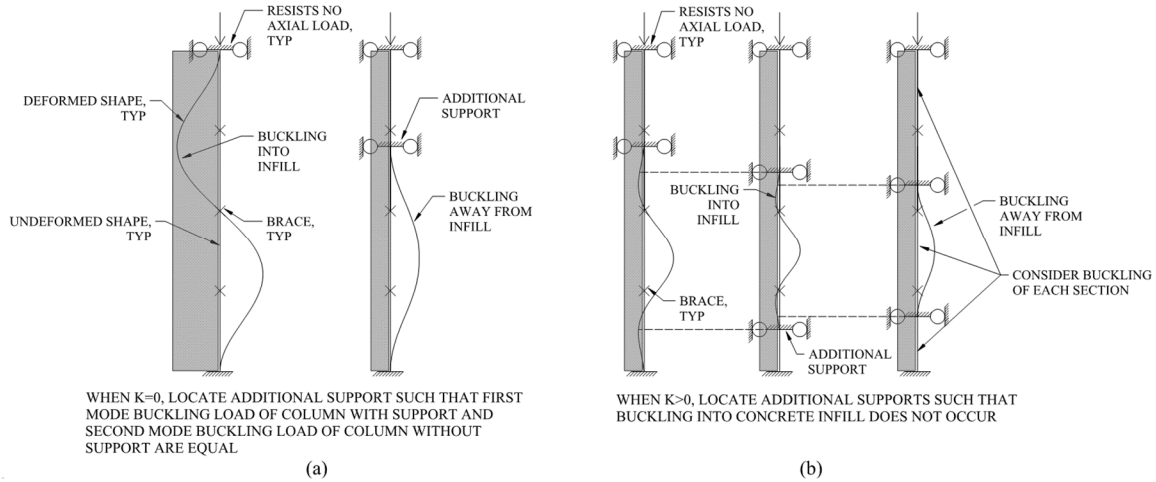

Figure 11: Second mode iterative buckling analysis for FF-3A.

The results of the buckling analysis for FF-3A are summarized in Fig. 12. Fig. 12 shows the normalized critical buckling load: P_{cr} / P_E, where P_E is the Euler buckling load between brace points: $P_E = \pi^2 \cdot E \cdot I / s^2$, on the ordinate and the normalized brace stiffness: $K \cdot s^3 / (E \cdot I)$, on the abscissa. The mode 1 – iterative and mode 2 – iterative buckling load solution are the governing buckling load for all brace stiffness values. As the brace stiffness increases, the governing buckling load increases, but does not exceed the mode 3 – lower bound or mode 6 – lower bound buckling load. Fig. 12 concludes that the column buckling load for FF-3A is governed by mode 1 – iterative for $K < 10 \cdot E \cdot I / s^3$ and the column buckling load is governed by mode - 2 iterative for $K \geq 10 \cdot E \cdot I / s^3$. The governing buckling load exceeds P_E for $K \geq 10 \cdot E \cdot I / s^3$ and exceeds $2 \cdot P_E$ for $K \geq 100 \cdot E \cdot I / s^3$.

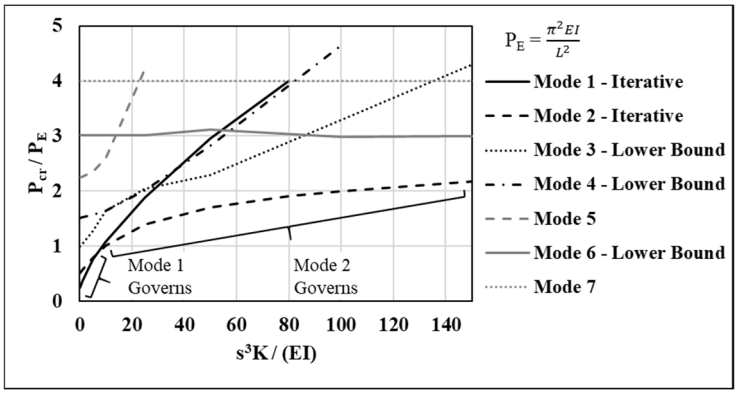

Figure 12: Buckling load versus brace stiffness for FF-3A.

3.5 Ideal Brace Stiffness

To determine the ideal brace stiffness for tie bars and shear anchors, a target buckling load must be established. The maximum buckling load which could be developed by the columns studied in this paper is $4 \cdot P_E$, corresponding to "fixed-fixed" conditions between brace points. This buckling load would require infinitely stiff braces. Zhang et al. (2020) found the mean effective length factor

for steel faceplates was 0.8. An effective length factor of 0.8 corresponds to a buckling load of $1.56 \cdot P_E$. The target buckling load for faceplates was chosen to be $2 \cdot P_E$ and the resulting ideal brace stiffness is $100 \cdot E \cdot I / s^3$.

The preceding discussion of FF-2A and FF-3A both found $100 \cdot E \cdot I / s^3$ to be the ideal brace stiffness. This is also the ideal brace stiffness for the column modeled with any number of intermediate braces greater than one. Fig. 13 shows that as the number of intermediate braces increases, the governing buckling load converges to the same value, for $K \geq 10 \cdot E \cdot I / s^3$. For a column with an even number of braces, the first buckling mode governs the buckling load. For a column with an odd number of braces, the second buckling mode governs the buckling load.

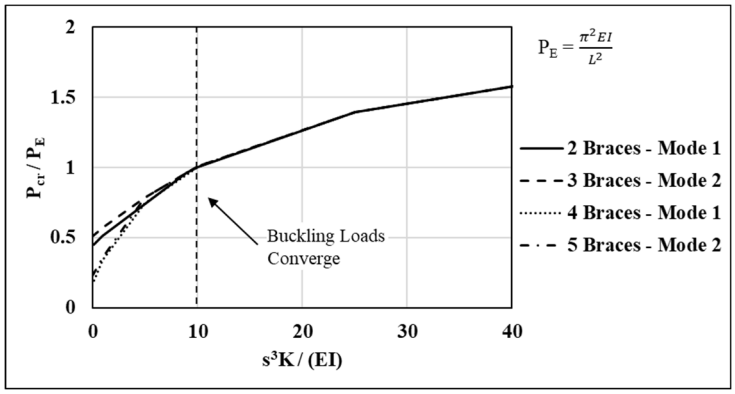

Figure 13: Converging buckling load versus brace stiffness of columns with multiple brace points.

3.6 Buckling of Steel Faceplates

The buckling behavior and ideal brace stiffness from the preceding discussion are applied to the buckling of steel faceplates for C-PSW/CF. For $K \geq 10 \cdot E \cdot I / s^3$, the faceplate is prevented from buckling away from the concrete infill over its entire length, see Fig. 14. A buckling analysis omitting the unilateral restraint of the concrete infill shows that the faceplate tends to buckle into the concrete infill for brace stiffness $K \geq 10 \cdot E \cdot I / s^3$. The concrete infill prevents the faceplate from buckling inwards, resulting in the concrete infill restraining the faceplate from buckling at multiple points along its length. The faceplate can buckle away from the concrete infill in between the contact points between the faceplate and concrete infill. The contact points separate the faceplate into shorter, separate segments to consider for a buckling analysis. The buckling load of the faceplate is the smallest buckling load from any of the resulting segments of the faceplate. The ideal brace stiffness for shear anchors and tie bars is $100 \cdot E \cdot I / s^3$, for the faceplate to reach a buckling load of $2 \cdot P_E$.

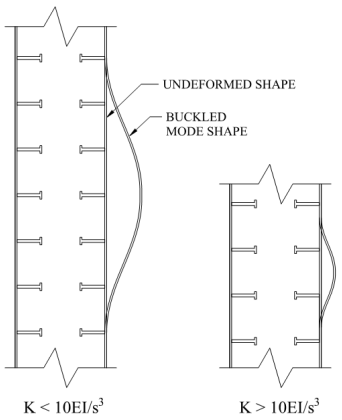

Figure 14: Governing buckling mode shapes.

The buckling mode shape of faceplates converges to the mode shape from the FF-2A mode 1 – iterative analysis, in Fig. 8. This buckled region of this mode shape extends above and below two adjacent rows of shear anchors or tie bars, see Fig. 14, for $K \geq 10 \cdot E \cdot I / s^3$. The buckling mode of faceplates for C-PSW/CF had not been previously identified by researchers. Zhang et al. (2014) speculated that local buckling occurred between adjacent rows of shear anchors. Zhang et al. (2020) provided experimental observations (photos) of local buckling in C-PSW/CF specimens. These pictures show the faceplate separating from the concrete infill over a region extending above and below two adjacent rows of shear studs.

The idea of local buckling occurring between adjacent rows of shear anchors from Zhang et al. (2014) does not contradict the governing mode shape presented in this paper. If the faceplate buckled between adjacent shear anchors and a finite brace stiffness were present, the tie bars and shear anchors would stretch due to the bracing (axial tension) force. This stretching force would extend the region of separation between the faceplate and concrete infill past the adjacent tie bars or shear anchors. The governing buckling mode presented in this paper and the idea of buckling between adjacent shear anchors form the same conclusion when tie bar and shear anchor deformation is considered. This axial flexibility of the tie bars and shear anchors is directly incorporated into the buckling analysis presented throughout this paper by modeling contact between the faceplate and concrete infill.

4. Numerical Modeling

Similar to the analysis completed by Winter (1958), initial imperfections were modeled in the faceplate to determine the required brace strength for design of shear anchors and tie bars. To estimate axial force demands in anchors at brace points, numerical (finite element) models of faceplates were created with SAP2000 (CSI 2014). The model represented a faceplate with two intermediate anchors. The total length of the faceplate model was three times the brace spacing ($3 \cdot s$). The width of each model was taken as 4in; the width of the model does not affect the outcome because all derivations were taken for a tributary width. Thin shell elements were used to model the faceplate, neglecting shear deformations. Intermediate anchors were modeled as linear springs and were distributed over the width of the faceplate. Boundary conditions enforced zero deflection and rotation at the ends of the faceplate. An initial out-of-straightness was modeled as the primary buckling mode shape determined from the preceding buckling analysis. The initial midspan displacement (Δ_0) was taken as s / 333. Three different faceplate geometries were modeled with

s/t_p of 11, 18, and 48 with t_p of 0.75in, 0.5in, and 0.25in, respectively. The SAP2000 model for s/t_p = 18 is shown in Fig. 15. For each faceplate geometry, three different values of the brace stiffness (K) were analyzed: one, two, and three times the ideal brace stiffness (K_{ideal}). The faceplate models were incrementally loaded in compression until an axial load of $2 \cdot P_E$ was applied. The midspan displacement and brace force were recorded at each load increment. The unilateral restraint was modeled by adding sliding "fixed" supports to the faceplate model and iteratively determining the location of the support, as done for the eigenvalue buckling analysis.

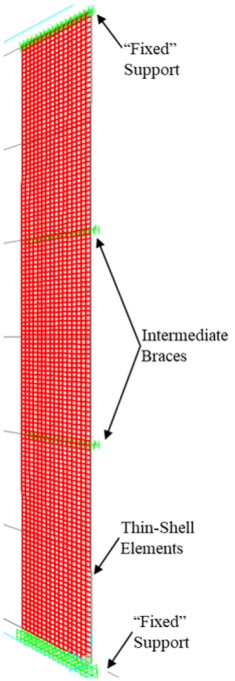

Figure 15: SAP2000 model of faceplate with two intermediate braces.

The applied axial load (P) versus midspan displacement (Δ) is plotted in Fig. 16 for each faceplate configuration analyzed. The applied axial load is shown as a normalized load (P / P_E), where P_E is the Euler buckling load ($P_E = \pi^2 \cdot E \cdot I / s^2$) and the midspan displacement is shown as a normalized displacement ($\Delta + \Delta_0$) / Δ_0, where Δ_0 is the initial midspan imperfection. The midspan displacement tends to infinity as the applied load approaches $2 \cdot P_E$, for $K = K_{ideal}$. For K = $2 \cdot K_{ideal}$, the midspan displacement after loading is less than 2.5 times the initial imperfection, when $P/P_E = 2$. The displacement after loading, when $P/P_E = 2$, decreases further for K = $3 \cdot K_{ideal}$.

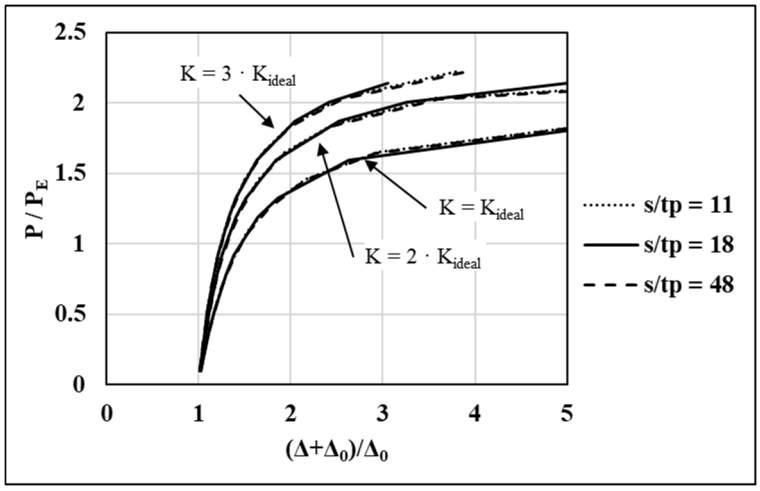

Figure 16: Applied axial load versus midspan displacement.

The applied axial load (P) versus resultant brace force (P_{br}) is plotted in Fig. 17 for each faceplate configuration analyzed. The applied axial load is shown as a normalized axial load (P / P_E), where P_E is the Euler buckling load ($P_E = \pi^2 \cdot E \cdot I / s^2$) and the resultant brace force is shown as a normalized force (P_{br} / P). The brace force tends to infinity as the applied load approaches $2 \cdot P_E$, for $K = K_{ideal}$. For $K = 2 \cdot K_{ideal}$, the brace force is 1.5% of the applied load, when $P/P_E = 2$. The brace force, when $P/P_E = 2$, decreases further for $K = 3 \cdot K_{ideal}$. Fig. 16 and Fig. 17 show that the brace stiffness affects the normalized load-deflection behavior of a faceplate, but the slenderness ratio does not.

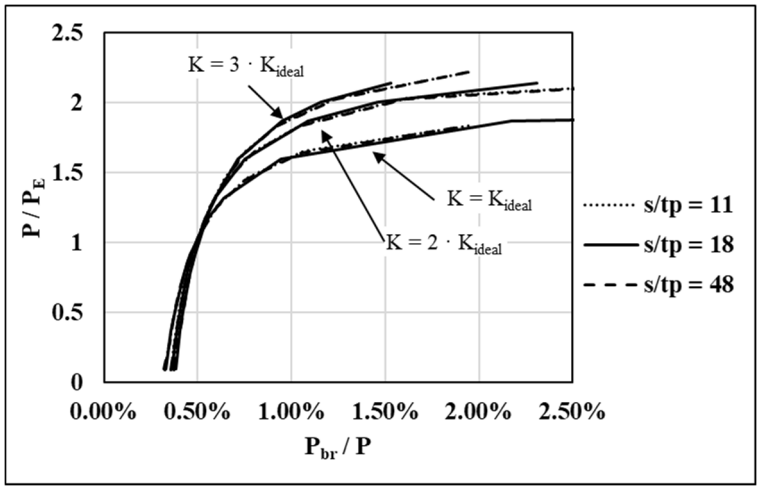

Figure 17: Applied axial load versus resultant brace force.

5. Strength and Stiffness Design Requirements

The ideal brace stiffness is the value of brace stiffness for a system which allows the bifurcation buckling load for that system to equal a targeted buckling load. The targeted buckling load for faceplates of C-PSW/CF was taken to be $2 \cdot P_E$. The ideal brace stiffness for shear anchors and tie bars to resist faceplate local buckling under compressive stress was determined to be $100 \cdot E \cdot I / s^3$. Twice the ideal brace stiffness has been accepted for design of column bracing in AISC 2016. Numerical modeling of faceplates demonstrated that a brace with twice the ideal brace stiffness

would allow the faceplate to develop the targeted buckling load with a displacement less than 2.5 times the initial out-of-straightness of the faceplate.

The required axial stiffness for shear anchors and tie bars is twice the ideal brace stiffness; this equals $200 \cdot E \cdot I / s^3$ or $200 \cdot P_E / (s \cdot \pi^2)$. Following AISC (2016), the axial load demand is substituted for the Euler buckling load. Faceplates are designed to develop their yield capacity; thus, the axial load demand for a faceplate with equal vertical and horizontal shear anchor spacing is $s \cdot t_p \cdot F_y$. This load demand is used in the axial stiffness requirement for shear anchors and tie bars given by Eq. 4.

$$K_{req} \geq \frac{200}{\pi^2} \cdot t_p \cdot F_y \tag{4}$$

where, K_{req} is the required axial stiffness of a shear anchor or tie bar, t_p is the faceplate thickness, and F_y is the faceplate yield stress.

Numerical modeling of faceplates demonstrated that the maximum brace force demand with K = $2 \cdot K_{ideal}$ was 1.5% of the applied load, for the assumed magnitude of initial out-of-straightness. The applied load to faceplates is limited to the yield capacity of the faceplate. The brace force demand is thus 1.5% of the yield capacity of the faceplate. The resulting axial strength requirement for shear anchors and tie bars is given by Eq. 5. The authors recommend considering all shear anchors and tie bars to be loaded simultaneously when determining their axial capacity.

$$F_{req} \geq 0.015 \cdot s \cdot t_p \cdot F_y \tag{5}$$

where, F_{req} is the required axial strength of a shear anchor or tie bar, s is the longitudinal and horizontal spacing between shear anchors and tie bars, t_p is the faceplate thickness, and F_y is the faceplate yield stress.

6. Conclusions

Concrete-filled composite plate shear walls (C-PSW/CF) consist of steel faceplates, tie bars, shear anchors, and concrete infill. Prior to being filled with concrete, tie bars provide lateral stability to the faceplates and resist shear buckling. After concrete infill is placed, tie bars and shear anchors resist buckling of the faceplate away from the concrete infill, among other functions. Shear anchors and tie bars act as point braces to resist faceplate buckling. Concrete infill acts as a unilateral support to the faceplate: preventing buckling into the concrete infill but providing no resistance to buckling away from the concrete infill. This paper presented a buckling analysis of steel faceplates of C-PSW/CF. The buckling analysis used an eigenvalue buckling method which iteratively applied boundary conditions to represent to unilateral restraint of the concrete infill.

For minimal brace stiffness, the faceplate will buckle away from the concrete infill over the entire height of the wall. This scenario is theoretical and is unrealistic in reality. The buckling analysis concludes that for brace stiffness greater than $10 \cdot E \cdot I / s^3$, the faceplate tends to buckle into the concrete infill, creating contact between the faceplate and the concrete infill. E is the elastic modulus of the faceplate, I is the moment of inertia of the tributary section for the brace, and s is the vertical spacing between shear anchors and tie bars. The contact provides restraint to the faceplate, separating the height of the faceplate into shorter segments over which buckling can

occur. The governing buckling mode results in the faceplate buckling over two adjacent rows of shear anchors or tie bars, regardless of the total number of shear anchor and tie bars or height of the wall. The separation between the faceplate and concrete infill extends above and below the adjacent rows of shear anchors and tie bars: creating axial forces in the braces. The buckling load of the faceplate increases as the brace stiffness increases; the buckling load reaches $2 \cdot P_E$ when the brace stiffness is $100 \cdot E \cdot I / s^3$. P_E is the Euler buckling load for the unbraced faceplate length. $100 \cdot E \cdot I / s^3$ is the ideal brace stiffness for this study; however, a greater brace stiffness than the ideal value is required for the buckling load to reach $2 \cdot P_E$ for a real structure with initial imperfections. If an initial imperfection of s / 333 is considered in the faceplate and twice the ideal brace stiffness is provided, the axial load demand on the shear anchors and tie bars, when the applied faceplate load is $2 \cdot P_E$, is 1.5% of the applied faceplate load.

The desired buckling load of faceplates for C-PSW/CF was set to be $2 \cdot P_E$. The ideal brace stiffness to achieve this buckling load was determined to be $100 \cdot P_E / (s \cdot \pi^2)$. To reach the desired buckling load in a real structure with initial imperfections, twice the ideal brace stiffness is recommended to be required for design of shear anchors and tie bars; however, P_E can be replaced by the yield capacity of the tributary faceplate section. If the horizontal and vertical shear anchor spacings are equal, the resulting required axial stiffness is $200 \cdot t_p \cdot F_y / \pi^2$, where t_p is the faceplate thickness, and F_y is the faceplate yield stress. The axial strength of shear anchors and tie bars to be required for design is recommend to be $0.015 \cdot s \cdot t_p \cdot F_y$.

The research completed in this paper applies directly to the design of steel faceplates, tie bars, and shear anchors for C-PSW/CF. Further research is being done to consider the effect of edge restraint to the faceplates due to boundary elements for C-PSW/CF. This further study will also apply to the design of concrete-filled steel box beams and columns. Current design provisions for these members assumes plate buckling behavior without tie bars or shear anchors: as the width of the section increases the required steel plate thickness increases to prevent local buckling before yielding. Use of tie bars or shear anchors for composite beams and columns would allow the design of wide members without increasing the required steel plate thickness.

Acknowledgments

This research was supported by the American Institute of Steel Construction (AISC) and Charles Pankow Foundation together through Grant Number RGA #06-16. Funding for the first author was provided by the Purdue Doctoral Fellowship Program at Purdue University.

References

AISC. 2016. "Specification for Structural Steel Buildings." *American Institute of Steel Construction*. Chicago, IL, USA.

CSI. 2014. (2014). "SAP2000 Integrated Software for Structural Analysis and Design" *Computers and Structures, Inc.* Berkeley, California.

Galambos, T.V., Surovek, A.E. (2008). "Structural Stability of Steel: Concepts and Applications for Structural Engineers." *John Wiley & Sons, Inc.* Hoboken, New Jersey, USA

Sio, J.F.A., Pinto da Costa, A., Simoes, F.M.F. (2017). "Buckling of unilaterally constraint columns by complementarity eigenvalue analysis." *International Journal of Solids and Structures*. 46-55: 106-107.

Varma, A.H., Shafaei, S., Klemencic, R. (2019). "Steel modules of composite plate shear walls: Behavior, stability, and design." *Thin-Walled Structures*, 145. https://doi.org/10.1016/j.tws.2019.106384

Winter, G. (1958). "Lateral Bracing of Columns and Beams." *Journal of the Structural Division,* ASCE, Vol. 84, No. ST3, pp. 1561-1-1,562-22.

Zhang, K., Varma, A.H., Malushte, S.R., Gallocher, S. (2014). "Effect of shear connectors on local buckling and composite action in steel concrete composite walls." *Nuclear Engineering and Design*, Elsevier, Vol. 269, pp. 231-239, Elsevier Science, http://dx.doi.org/10.1016/j.nucengdes.2013.08.035

Zhang, K., Seo, J., Varma, A.H. (2020). "Steel-Plate Composite Walls: Local Buckling and Design for Axial Compression." *Journal of Structural Engineering*, Vol. 146, No. 4, https://doi.org/10.1061/(ASCE)ST.1943-541X.0002545